

This article was downloaded by: [Tomsk State University of Control Systems and Radio]

On: 21 February 2013, At: 11:31

Publisher: Taylor & Francis

Informa Ltd Registered in England and Wales Registered Number: 1072954  
Registered office: Mortimer House, 37-41 Mortimer Street, London W1T 3JH, UK



## Molecular Crystals and Liquid Crystals

Publication details, including instructions for authors and subscription information:

<http://www.tandfonline.com/loi/gmcl16>

### Observations of Sm C Layer Undulations and Sm C Edge-Dislocations in NOBA Films

H. P. Hinov<sup>a</sup> & M. Petrov<sup>a</sup>

<sup>a</sup> Institute of Solid State Physics, Boul. Lenin 72, Sofia, 1184, Bulgaria

Version of record first published: 20 Apr 2011.

To cite this article: H. P. Hinov & M. Petrov (1983): Observations of Sm C Layer Undulations and Sm C Edge-Dislocations in NOBA Films, *Molecular Crystals and Liquid Crystals*, 100:3-4, 223-251

To link to this article: <http://dx.doi.org/10.1080/00268948308075354>

PLEASE SCROLL DOWN FOR ARTICLE

Full terms and conditions of use: <http://www.tandfonline.com/page/terms-and-conditions>

This article may be used for research, teaching, and private study purposes. Any substantial or systematic reproduction, redistribution, reselling, loan, sub-licensing, systematic supply, or distribution in any form to anyone is expressly forbidden.

The publisher does not give any warranty express or implied or make any representation that the contents will be complete or accurate or up to date. The accuracy of any instructions, formulae, and drug doses should be independently verified with primary sources. The publisher shall not be liable for any loss, actions, claims, proceedings, demand, or costs or damages

whatsoever or howsoever caused arising directly or indirectly in connection with or arising out of the use of this material.

# Observations of Sm C Layer Undulations and Sm C Edge-Dislocations in NOBA Films

H. P. HINOV and M. PETROV

*Institute of Solid State Physics, Boul. Lenin 72, Sofia 1184, Bulgaria*

(Received August 2, 1982; in final form May 9, 1983)

Sm C layer undulation instabilities produced by first and second-order effects have been obtained after the rapid cooling of thin (10–26  $\mu$ m) homeotropic and twisted nematic NOBA films. The Sm C dilation modulus  $B$  has been approximately calculated to be around  $0.32 \times 10^{-4}$  erg/cm<sup>3</sup> and the larger value of the Sm C elastic coefficient  $A_{21}$  relative to that of  $A_{12}$  has been demonstrated.

A number of novel, directly-observable Sm C edge-dislocation lines (or walls) have been obtained after the rapid cooling of electrically-deformed twisted nematic NOBA films. A physical model explaining their creation has been given. The possible relaxation of the dislocation walls into Néel walls with a partial twist and further into alternating nuclei with strength  $\pm 1$  has not been observed, possibly due to the larger value of  $A_{21}$  relative to that of  $A_{12}$ . Possibilities for storage applications have briefly been discussed.

## I. INTRODUCTION

Smectic A, B, C, etc. phases of liquid crystals (LCs) with nematic to smectic A (N–Sm A), nematic to smectic B (N–Sm B) and nematic to smectic C (N–Sm C), etc., phase transitions have usually been obtained and investigated after a slow cooling of the well-aligned nematic phase down to the corresponding smectic phase. On the other hand, they can be created after slow or rapid cooling of previously deformed nematic films. For instance, the nucleation of a Sm A phase from an initially bent nematic CBOOA has been investigated in detail by Cladis and Torza<sup>1</sup> who related the Sm A textures observed with the scattering properties of the well-known Kahn's thermo-optical display devices.<sup>2</sup> In addition, the growth of a Sm A phase after a rapid cooling of electrically-deformed planar nematic CBOOA films has been studied

in a technically simple manner by Hinov.<sup>3</sup> Of interest is that the magnitude of the voltage being applied across the films under study was changed between  $3U_{th}$  and  $30U_{th}$ , where  $U_{th}$  is the Freedericksz threshold voltage. Under these conditions the Sm A phase grew first from the well-aligned nematic in the middle part of the cells and after that from the two strongly-deformed nematic boundary regions.

The cooling of previously-deformed Ns down to the smectic phase may first give important information about smectic surface forces,<sup>3</sup> hitherto insufficiently investigated and may secondly aid in the obtaining of a number of homogeneous and stable smectic scattering textures, which are governed by surface forces and which contain in their structure defects related to both translational symmetry breaking (dislocations) and to rotational symmetry breaking (disclinations).<sup>3</sup> Such experiments should be carried out with Sm LCs nucleating either all at once in the entire cell or at first in the middle part of the sample, which is the most important case. To nucleate the smectic phase first in the middle part of the samples without utilizing a special kind of temperature gradient (it is well-known that the smectic phases start usually to nucleate at the glass plates where the nucleation energy is zero) it is necessary to use a previously-deformed nematic phase having pronounced pretransitional behaviour around the N–Sm A, N–Sm B, and N–Sm C, etc., phase transitions that are accompanied first at all by the creation of pretransitional stripe-like domains.<sup>1</sup>

This paper deals with the formation of a Sm C phase after the rapid cooling of electrically-deformed planar, hybrid (homeotropic-planar) and twisted nematic NOBA films. During the experimental investigations, a number of either well-known or novel Sm C textures are obtained giving important information about the possible matching of the Sm C liquid crystal, one of which is nucleated in the middle part of the samples, and the other formed in the boundary regions. The possible ways for the Sm C phase growing, including the orientation of the Sm C molecules and the position of the Sm C planes were clarified as well as the crucial role of the initial twist in the nematic phase and the strength of the voltage applied across both the nematic and Sm C phases for the creation of various Sm C textures were demonstrated. Moreover, the possible role of the surface forces has been discussed in detail (let us note that the competition between the surface forces and the bulk forces has not been investigated up to now either theoretically or experimentally). Finally, the Sm C layer undulations observed permitted first a numerical estimation of the dilation modulus  $\tilde{B}$  of the Sm C liquid crystal NOBA under study which has been compared to that already obtained by Johnson and Saupe for the case of the liquid

crystal 5BA6 with a Sm A to Sm C phase transition,<sup>4</sup> and second unambiguously pointed out the larger elastic coefficient between  $A_{12}$  and  $A_{21}$ .

## II. EXPERIMENTAL RESULTS

### A. Compound and sample preparation

The liquid crystal under study, NOBA (*p*-*n*-nonyloxybenzoic-acid), with a nematic phase between 117°C and 143°C and a Sm C phase between 117°C and 94°C is characterized by well-defined pretransitional stripes around the N–Sm C phase transition. The characteristic tilt of the NOBA Sm C molecules with respect to the Sm C planes has been measured to be around 45° within the entire Sm C temperature interval.<sup>5</sup>

The LC was first introduced between two NESA coated glass plates separated by mylar spacers 10 to 50 microns thick in its isotropic phase after being warmed by a regulated electric heater. The sample was then placed on the stage of a NU 2 microscope. The massive metal lateral holder stored the thermal energy such that the cooling rate of nearly 15°C/min was sufficient for the performance of the experiment. This manner of cell preparation has several advantages resulting in possibilities for achieving high horizontal temperature gradients in the electrode planes, which permits the easy observation of pretransitional effects around the N–Sm C phase transition, the investigation of a large area (several cm<sup>2</sup>) of the LC and photography of the LC structures with objectives having small focal lengths (magnifications  $\times 400$ ).

During the experimental investigations a number of planar, homeotropic-planar and twisted N NOBA films were cooled down to the Sm C phase in the presence of an a.c. electric field with differing strength. The planar and twisted orientation of the LC molecules were obtained by SiO treatment of the electrodes under vacuum evaporation whereas the homeotropic orientation was achieved by lecithin coating of the glass plates.

### B. Thermal distribution in the LC cells under investigation

The thermal distribution in the LC cells under study has been discussed in detail elsewhere.<sup>3</sup> In such cells one notes a strong temperature gradient in the electrode planes being directed from the lateral metal holders storing thermal energy to the middle part of the cells.

On the other hand, it is reasonable to accept a nearly homogeneous temperature distribution along  $Z$ , i.e. normal to the glass plates. This assumption is especially true for the thin LC cells being investigated in our experiment (one can obtain a nearly correct picture for the temperature distribution in thin LC cells by means of the typical scattering properties of widely-used short-pitch cholesterics: for instance, the clear colours produced by such cholesteric LCs 10–20 microns thick unambiguously pointed out the nearly constant temperature over the entire LC layer even for samples heated from below<sup>6</sup>—the temperature gradient would widen the frequency range of the selective reflection of the light, which is related to the observation of iridescent colours, as has been pointed out by Hajdo and Eringen.<sup>7</sup> One notes, however, a significant temperature gradient between the outer sides of the glass plates confining the LC, which clearly shows the great importance of the thermal properties of the glass plates, depending on their thickness and thermal conductivity, etc.). In addition, we have observed very often a well-defined Schlieren texture and Bloch walls<sup>8–10</sup> in the nematic phase of NOBA existing not very close to the isotropic phase. The degeneracy in the LC alignment implies the existence of thin isotropic layers near to the glass plates; this unambiguously points out the higher temperature in these regions.

### C. Electric field application

The dielectric properties of the NOBA LC under study in both the nematic and Sm C phases as well the temperature dependence of the dielectric tensor elements have been insufficiently investigated up to now. The preliminary experimental results obtained by Kuvatov *et al.*<sup>11,12</sup> and some interesting results obtained by Chou and Carr<sup>13</sup> clearly show first that the dielectric anisotropy is positive in the nematic phase and negative in the Sm C phase and second, that their temperature variations in both phases are negligible (see Figs. 6 and 7 in Ref. 13). In addition, it is well-known that Sm C LCs are biaxial with differing magnitudes for the three principal dielectric tensor elements. However, the experimental results obtained by Kuvatov *et al.* unambiguously pointed out the nearly equal value of the transversal dielectric permittivities characterizing the low-frequency dielectric properties of NOBA in planes perpendicular to the long axis of the molecules, i.e. the Sm C liquid crystal NOBA is practically one uniaxial Sm C medium. The values of the dielectric anisotropy of the N and Sm C phases have been determined to be +0.028 and –0.025 ( $f = 10$  kHz), respectively.

A high frequency voltage ( $f = 10$  kHz) with a strength between  $U_{th}$  (the threshold voltage  $U_{th}$  was in the range of 26–30  $V_{eff}$  depending on the impurity content) and  $15U_{th}$  was applied across the LC films under study in both the N and Sm C phases in order to obtain complete orientation of the nematic molecules in the middle part of the samples and two strongly-deformed LC nematic regions at the glass slides. The frequency of the applied electric field was sufficiently high for ensuring the orienting action of the dielectric torques without any hydrodynamic movement of the fluid.

#### D. Microscopic observations

The Sm C phase of the liquid crystal NOBA has been nucleated after a rapid cooling of either non-deformed or electrically-deformed PLANAR and TWISTED nematic films. The experimental results obtained for these two complementary cases are very important for understanding the novel Sm C textures observed.

(1) Sm C phase obtained after the rapid cooling of non-deformed planar and twisted nematic NOBA films.

The rapid cooling of thin planar nematic NOBA films of 10–26 microns down to the Sm C phase often led to the formation of many local Sm C monodomains separated by  $\pi$ -inversion walls. The nucleated Sm C blurred Schlieren texture in thick cells, however, was not controlled by the action of the surface forces. The rapid cooling of thin twisted nematic NOBA films of 10–26 microns thick, on the other hand, led to the formation of a number of pretransitional stripes and Sm C patterns as follows:

(a) pre-transitional parallel stripes very similar to those already observed and investigated by Cladis and Torza in Sm A<sup>1</sup> and by Scheffer *et al.* in Sm C droplets.<sup>14</sup> In cells with a thickness well above 10–15 microns, cone-like pretransitional domains were observed due to the larger temperature gradient in the electrode plane.<sup>1,14</sup>

(b) Sm C Schlieren texture with one-dimensional undulation instability (stripes) at higher temperatures in the Sm C interval (Figure 1), as observed and investigated in detail by Johnson and Saupe in LCs with Sm A–Sm C phase transition<sup>4</sup> (these stripes have been occasionally observed also by Bartolino *et al.*<sup>15</sup>, Kumar<sup>16</sup> and Bourdon *et al.*<sup>17</sup> in various experiments on LCs with Sm A to Sm C phase transition) and two superimposed one-dimensional instabilities at low temperatures in the Sm C interval which have already been called a cross-hatched pattern by Johnson and Saupe<sup>4</sup> (Figure 2).

(2) Sm C phase obtained after rapid cooling of electrically-deformed planar and twisted nematic NOBA films.

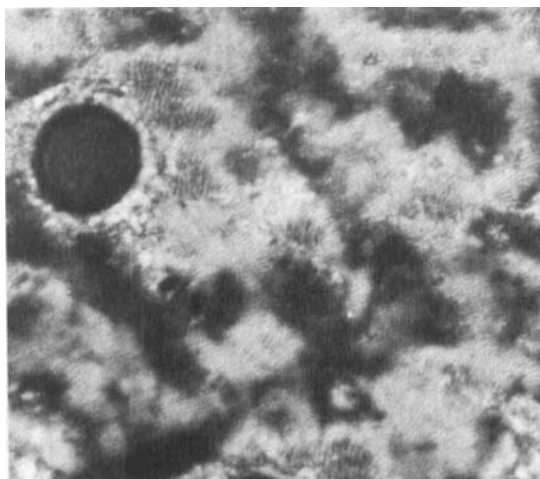


**FIGURE 1** Smectic C Schlieren texture with Sm C layer undulation instabilities in a thin (26 microns) NOBA films produced by second-order effects after rapid cooling of the twisted nematic phase. These Sm C patterns usually appear in the upper temperature range of the Sm C phase. Crossed nicols, the short side of the photo corresponds to 480 microns.



**FIGURE 2** Smectic C Schlieren texture with two superimposed Sm C layer undulation instabilities (cross-hatched patterns<sup>4</sup>) in a thin (26 microns) NOBA film produced by first and second-order effect after rapid cooling of the twisted nematic phase. These Sm C patterns usually appear in the lower temperature range of the Sm C phase. Cross nicols, each side of the photo corresponds to 510 microns.



The growth of the Sm C phase from electrically-deformed planar nematic NOBA films upon rapid cooling was in the form of well-defined Sm C local monodomains with different orientations of the Sm C molecules and the Sm C planes (Figure 3). The stacking of the local Sm C monodomains gave a number of discontinuous lines already discussed by Demus and Richter to be probable inversion walls.<sup>18</sup> One may often observe weakly contrasting lines which follow the orientation of the Sm C layers and which probably represent the imperfections of the Sm C LC illuminated between parallel or crossed nicols clearly shows the various  $\varphi$ -orientation of the Sm C molecules either in some of the Sm C monodomains or in the Sm C monodomains themselves when passing from one monodomain to another.

The growth of the Sm C phase from electrically-deformed twisted nematic NOBA films upon cooling, however, was quite different. At low voltages applied to both N and Sm C phases in the range of  $20 V_{\text{eff}}$  to  $60 V_{\text{eff}}$ , a well-defined Schlieren texture with Johnson-Saupe's stripes has been observed after the pre-translational stripes. The application of this low a.c. voltage (the threshold voltage as noted was in the range of  $16\text{--}20 V_{\text{eff}}$ , depending on the impurity content) did not remove the Sm C layer undulations which existed in the voltageless LC state as well. This voltage, however, led to the slight increase of the stripe period. The application of voltage above  $100 V_{\text{eff}}$  across both the N and Sm C phases gave rise to the disappearance of the Schlieren texture with the stripes and to the formation of many Sm C local monodomains with different irregularities of the Sm C planes (Figure

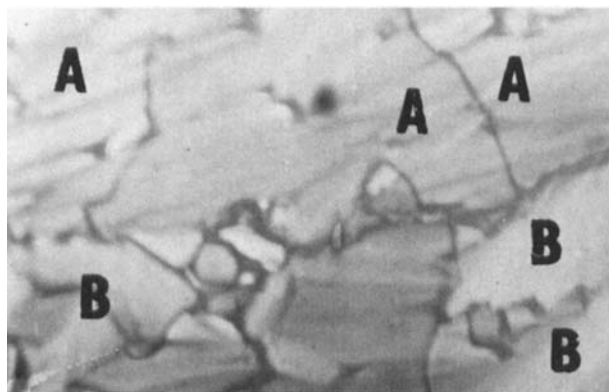
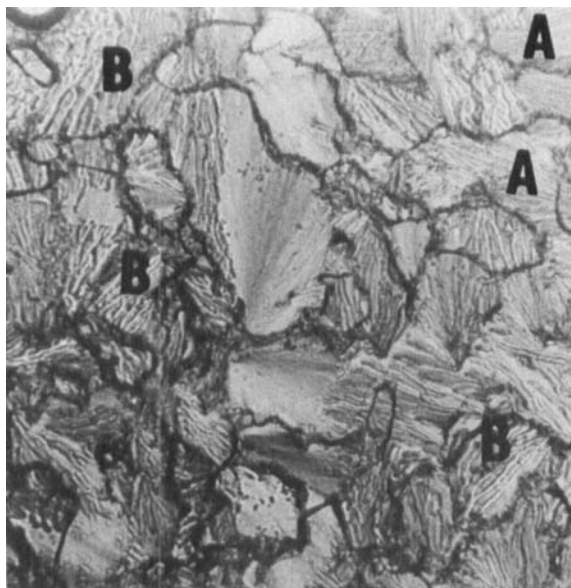
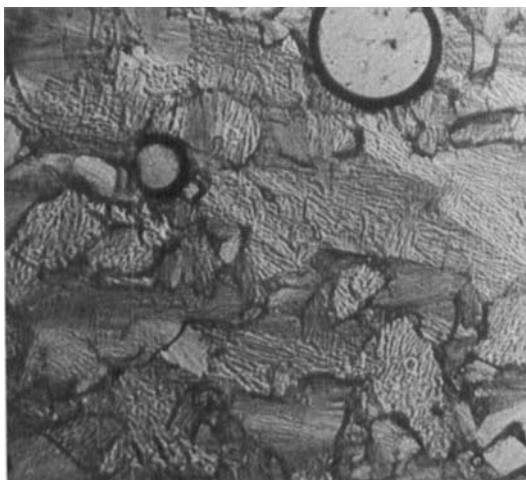


FIGURE 3 Smectic C local monodomains with weakly-contrasting lines designated by A and smectic C local homogeneous monodomains designated by B, formed after rapid cooling of a thin (26 microns) electrically-deformed planar nematic NOBA film. Parallel nicols, the short side of the photo corresponds to 400 microns.



**FIGURE 4** Smectic C local monodomains with various tilted-inversion walls designated by A and edge-dislocation lines designated by B, formed after rapid cooling of a thin (26 microns) electrically-deformed twisted NOBA films. Parallel nicols,  $U_{eff} = 220$  V,  $f = 10$  kHz, each side of the photo corresponds to 590 microns.



**FIGURE 5** Smectic C local monodomains with edge-dislocation lines formed after rapid cooling of a thin (26 microns) electrically-deformed twisted nematic NOBA films. Parallel nicols,  $U_{eff} = 280$  V,  $f = 10$  kHz, the short side of the photo corresponds to 500 microns.

4). The further increase of the voltage up to 300  $V_{\text{eff}}$  (which was achievable in our experiment) led to a significant decrease in their period (Figure 5). The crude measurements of the irregularity period gave roughly the law  $d \sim 1/E$ , where  $d$  is the irregularity period and  $E$  is the strength of the electric field applied across both the N and Sm C phases (Figure 6).

It is important to stress that the electric field was capable of influencing the irregularity behavior even in the Sm C phase. For instance, the increase of the voltage applied across the Sm C film above a certain threshold value caused a significant change in the irregularity period, which decreased by about two times and vice versa the decrease in the voltage led to a corresponding increase in the irregularity period. Occasionally the change in the electric field magnitude led to a defocusing of the Sm C irregularities as well. Moreover, the total removal of the voltage was accompanied also by a slight increase in the irregularity period which clearly pointed out that the irregularities exist even in the voltageless Sm C state as a storage mode. We shall not study here in detail the irregularity behavior under the influence of the electric field since this complicated problem requires further investigation. We shall use, however, these experimental results to interpret the possible orientation of the Sm C molecules and layers.

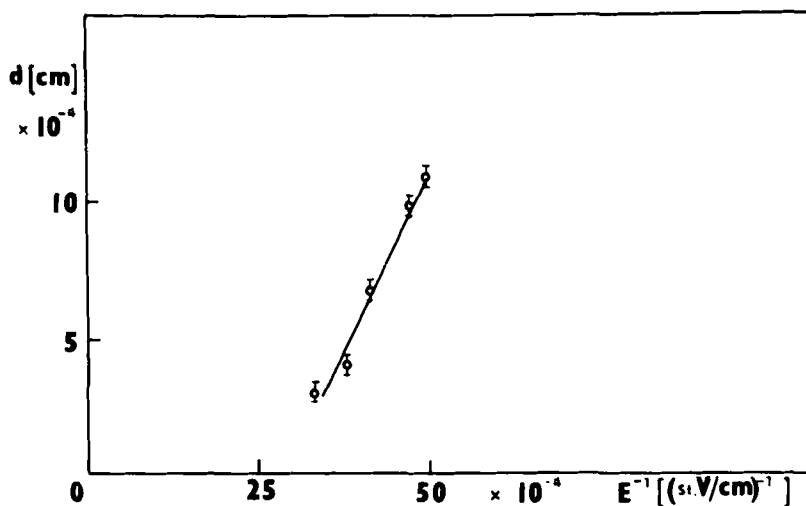


FIGURE 6 The edge-dislocation period ( $d$ ) versus the inverse strength of the electric field ( $1/E$ ) applied across both the N and Sm C phases. One notes the crude law  $d \sim 1/E$ .

As far as high voltages, well above  $300 V_{\text{eff}}$ , are concerned, we may say that with such high electric fields (unattainable in our experiment) a number of well-defined Sm C single crystals should be formed due to the eventual overcoming of the surface forces in the nematic phase.

### III. DISCUSSION

#### (1) Johnson-Saupe's stripes

(a) Influence of the thickness of the films under study, initial orientation of the nematic phase and the surface anchoring of the Sm C phase.

The formation of Johnson-Saupe's stripes in LCs with N to Sm C phase transition may give valuable information about the magnitude of the dilation modulus and about some of the elastic constants of this class of LCs. Of interest are the possible ways for the easy and reproducible experimental creation of these Sm C layer instabilities.

All the Sm C layer instabilities observed up to now have been obtained after a rather rapid cooling of N or Sm A films with different thicknesses determined by teflon or other hard-compressible spacers down to the Sm C phase. The stripes always exist in Sm C Schlieren textures characterized by Sm C layers parallel to the glass plates with  $\pm 1$  nuclei perpendicular to the glass plates and/or  $\pi$ -inversion bulk walls.<sup>18,19</sup> Consequently, the projection of the Sm C molecules being tilted relative to the glass plates can continuously change their direction in the plane of the electrodes.

The role of the surface anchoring of the Sm C films is of significance as well. It is well-known from the literature that the strong  $\theta$ -polar and  $\varphi$ -azimuthal anchoring of the Sm C molecules at the boundaries (Figure 7), achieved for instance by means of thin SiO film deposition under vacuum evaporation, can govern the formation of local Sm C monodomains with vertical or oblique orientation of the Sm C planes relative to the glass plates (planar position of the Sm C molecules).<sup>18-22</sup> The rubbing technique, on the other hand, can determine only the projection of the Sm C molecules on planes, parallel to the electrodes (strong  $\varphi$ -azimuthal, weak  $\theta$ -polar surface anchoring).<sup>23-26</sup> In addition, the rubbing technique may determine the initial twisting of the molecules in the Sm C phase<sup>24</sup> (a twisting of the Sm C molecules from layer to layer has been observed by Sakagami *et al.* in Sm C spherulities as well<sup>27</sup>).

It is clear that strong surface forces can determine various orientations of the Sm C molecules. However, this is only possible for thin

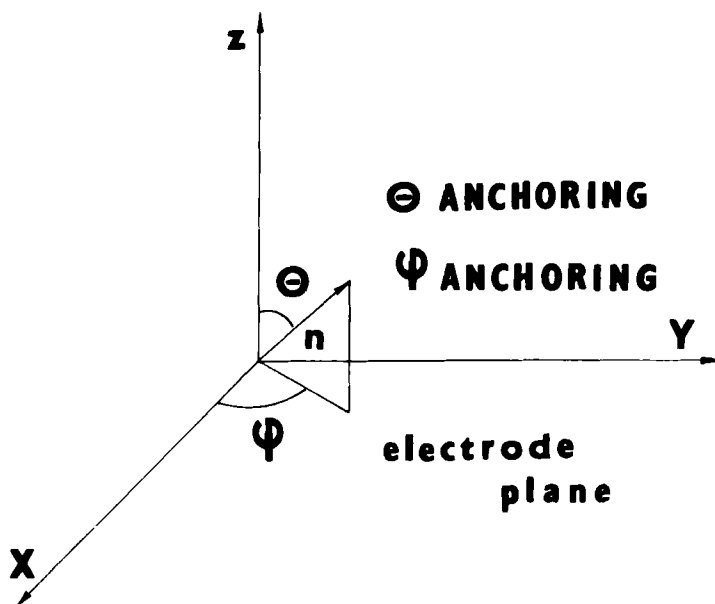


FIGURE 7 Schematic representation of the  $\theta$ -polar and  $\phi$ -azimuthal anchoring of N and Sm C molecules.

LC cells with a thickness in the range of 10–20 microns. For example, the experimental investigations of Price and Bak on Sm A films<sup>28</sup> unambiguously pointed out a 20–50 microns penetration depth of the Sm A surface forces into Sm A films under study which is surprisingly below the penetration depth of the surface forces into N films measured to be several hundreds microns.<sup>29,30</sup> It seems that this small penetration depth of the surface forces into Sm A films is due not to their weakness but rather to the very bulk forces of the Sm LCs which are able to overcome the surface forces even for relatively thin smectic films in the range of 30–50 microns.

Our experimental observations clearly show that Sm C layer undulations are not possible for the case of either vertical or oblique Sm C planes relative to the glass plates (Figure 8). It is easy to understand that the thermo-mechanical forces leading to the formation of Johnson-Saupe's stripes are not capable of causing such Sm C layer undulations in these cases due to the small lengths of the Sm C layers.

The experimental results have shown that Sm C Schlieren textures with stripes are easily obtainable after a rapid cooling of twisted N films. It is more difficult, however, to obtain a Sm C Schlieren texture

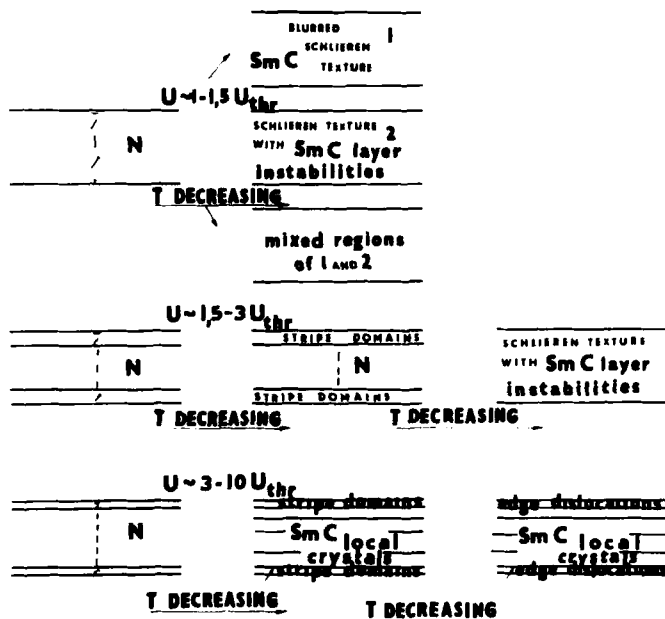
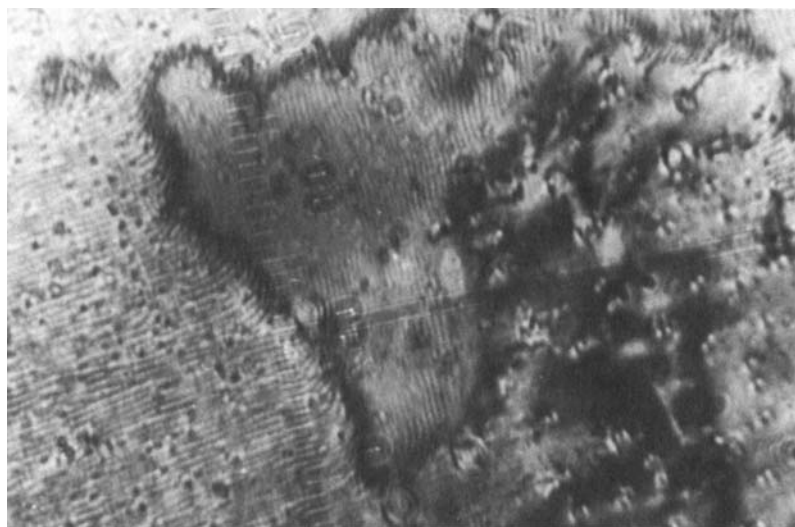


FIGURE 8 Schematic representation of various N and Sm C textures obtained before and after rapid cooling of twisted nematic NOBA films, respectively.

after the rapid cooling of planar N films. Sm C Schlieren textures with stripes can be easily created from homeotropic nematic films upon cooling as well.<sup>19</sup> Accordingly, such patterns were obtained during our experimental investigations after the rapid cooling either of hybrid-aligned nematic films with planar orientation of the molecules at one of the boundaries and homeotropic orientation at the other, or by the rapid cooling of homeotropic nematic films.

Nice Schlieren textures with closed bulk inversion walls and stripes were obtained after the rapid cooling of homeotropic nematic NOBA films, when the glass plates had previously been rubbed to prevent full-azimuthal degeneration of the orientation of the Sm C molecules (Figs. 9a and 9b). In a number of cells very nice stripes were obtained in a large area and only the existence of isolated focal-toric domains already studied by Perez *et al.*<sup>31</sup> and by Bourdon *et al.*<sup>17</sup> has indicated the planar position of the Sm C planes (Figure 10).

It seems that the essential reasons responsible for the formation of Johnson-Saupe's stripes in LCs with Sm A to Sm C phase transition<sup>4</sup> coincide with those leading to the creation of the same stripes in LCs with N to Sm C phase transition. Our experimental observations,



(a)



(b)

**FIGURE 9** Formation of a Schlieren Sm C texture consisting of  $\pi$ -inversion bulk walls with pronounced Sm C layer undulations after rapid cooling of a thin (26 microns) homeotropic nematic NOBA film: (a) beginning of the Sm C layer undulations; (b) final undulation of the Sm C layers;  $P\ 45^\circ A$ , the short side of the photo corresponds to 330 microns.

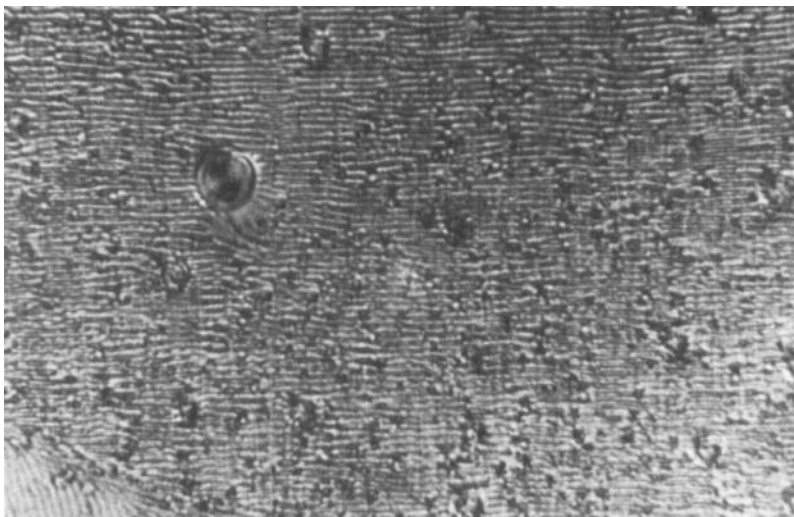


FIGURE 10 Formation of a Schlieren Sm C texture consisting of  $\pi$ -inversion bulk walls with pronounced Sm C layer undulations after rapid cooling of a thin (26 microns) homeotropic nematic NOBA film, P 45 °A. The glass plates have been previously rubbed in a direction which coincides with that of the long axis of the stripes. One notes circular confocal domains as well. The short side of the photo corresponds to 330 microns.

however, clearly pointed out that the stripes obtained from a homeotropic nematic phase upon cooling down to the Sm C phase are parallel to the  $C_2$  axis,<sup>4</sup> i.e., they have been caused by second-order effects related to a strong coupling between the layer curvature and the tilt orientation of the Sm C molecules.<sup>4</sup> In such films the Sm C stripes produced by first-order effects characterized without any coupling between the layer curvature and the tilt orientation<sup>4</sup> were not observed even at low temperatures in the Sm C phase: at such temperatures we observed only strong transversal undulations of the stripes (Figs. 9b and 10) (let us recall that the first-order stripes do exist in Sm C Schlieren textures formed from twisted nematic NOBA films upon rapid cooling).

(b) An approximate determination of the NOBA dilation modulus  $\tilde{B}$ .

The Sm C first-order undulation instability of an LC with Sm A to Sm C phase transition permits a simple determination of their dilation modulus  $\tilde{B}$ .<sup>4</sup> For this purpose the well-known expression for the “penetration” length of the Sm C layer undulation should be used:

$$\Lambda = (C_1/\tilde{B})^{1/2} \quad (1)$$



where  $\tilde{B}$  is the dilation modulus,  $C_1$  is the effective elastic coefficient and  $\Lambda$  can be determined from the stripe period according to the following formula:

$$\Lambda = \frac{\lambda_c^2}{4\pi d} \quad (2)$$

where  $\lambda_c$  is the period of the stripes produced by first-order effects (let us stress that these stripes have the greater period in the cross-hatch patterns<sup>4</sup>).

Taking into account the stripe period being around 7.6 microns (see Figure 2) and the mean value of the effective elastic coefficient  $C_1$  expected to be in the range of  $10^{-6}$  dynes we calculated the following approximate magnitude for the NOBA dilation modulus  $\tilde{B}$ :

$$\tilde{B}_{\text{NOBA}} \approx 0.32 \times 10^{+4} \text{ erg/cm}^3$$

Comparing the value of this coefficient with that obtained for the 5BA6 liquid crystal<sup>4</sup> measured to be around  $10^{+5}$  erg/cm<sup>3</sup> we can make, with some caution, the conclusion that LCs with N to Sm C phase transition have a dilation modulus  $\tilde{B}$  which is lower relative to that of LCs with N-Sm A-Sm C, etc., phase transitions. We find some justification for this important, according to us, conclusion in the experimental finding that electrohydrodynamic domains have not yet been observed in LCs with N-Sm A-Sm C, etc., phase transitions,<sup>32</sup> probably in part due to the hard compressibility or dilatation of their Sm C layers. Moreover, de Vries pointed out that different kinds of forces should act in these two types of liquid crystals.<sup>33</sup>

(c) Determination of the larger elastic coefficient between  $A_{12}$  and  $A_{21}$ .

A comparison between the experimental values obtained for the "penetration" length of both the first-order and second-order Sm C layer undulations according to the formulae:

$$\Lambda_1 = (A_{12}/\tilde{B})^{1/2} \quad (3)$$

and

$$\Lambda_2 = (A_{21} - C_2^2/B_2)^{1/2}(\tilde{B})^{-1/2} \quad (4)$$

( $A_{12}$ ,  $A_{21}$ ,  $C_2$  and  $B_2$  are the elastic coefficients given in Orsay notation<sup>34</sup>,  $\tilde{B}$  is the dilation modulus) can easily give the larger elastic coefficient between  $A_{12}$  and  $A_{21}$ .

Our experimental observations for the NOBA case clearly point out an experimental equality in the value of the periods of the two kinds of stripes (let us recall that the experimental value of the period of the second-order Sm C layer instabilities should be doubled):

$$\lambda_{c_1} \approx \lambda_{c_2}$$

This experimental finding together with the positive value of the elastic coefficient  $B_2$  (see for example the Sm C energy expression written by Kléman and Lejcek<sup>35</sup>) clearly point out that  $A_{21}$  IS THE LARGER NOBA ELASTIC COEFFICIENT between  $A_{12}$  and  $A_{21}$ :

$$A_{21} > A_{12}$$

## (2) Edge-dislocation lines

A plausible interpretation of the irregularities obtained during our experimental research (Figures. 4 and 5) has required a careful comparison of all the Sm C defects proposed and explained from a theoretical point of view<sup>21,36-38</sup> with those observed during the experimental investigations of the Sm C phase up to now<sup>17,18,19,21</sup> etc. Following this path our first attempts for explaining the objects observed were in part successful since we were able to interpret only some of them. For instance, a number of the Sm C monodomains were created with different orientations of the Sm C molecules, as revealed by the corresponding orientation of some of the irregularities interpreted to be different types of inversion tilted walls, which are designated by A in Figure 4 (note again that the thick lines with a number of  $\pm 1$  nuclei separate adjacent Sm C monodomains with different orientations of the Sm C layers in accordance with the interpretation given by Demus and Richter<sup>18</sup>). The wall lines in agreement with Demus and Richter's discussion<sup>18</sup> point out the orientation of the Sm C layers relative to one axis chosen on the glass plates, say, for example, the rubbing axis.

Another part of the irregularities has been interpreted in an analogy with the already observed and investigated in detail edge-dislocation lines (or tilted walls of dislocations) in Sm A liquid crystal.<sup>39-41</sup> For instance, some of the lines or stripes designated by B in Figure 4 and all the imperfections observable in Figure 5 have been interpreted by us to be possible edge-dislocations of the Sm C layers (indirectly observable Sm C edge-dislocations with a very small Burger's vector equal to one unit of smectic layer thickness in wedge-shaped samples have already been investigated in detail by Meyer, Lagerwall and Stabler in LCs with N-Sm A-Sm C, etc., phase transitions<sup>42-45</sup>).

Directly observable edge-dislocations have already been discovered in the Sm C liquid crystal DOBCP in 1971 by Lefèvre *et al.*<sup>46</sup> which were designated as an “epi” structure. Furthermore, the birefringence measurements performed by these authors in N and Sm C phases unambiguously pointed out the nearly equal LC orientation for this “epi” structure relative to that of the nematic phase.

The clarification of the Sm C orientation in the middle part of the samples under study as well as in the boundary regions can significantly aid in understanding of the possible physical reasons responsible for the creation of DIRECTLY-OBSERVABLE edge-dislocations in Sm C LCs. Let us study these cases in more details.

(a). Alignment of the Sm C phase in the middle part of the samples being investigated.

Our assumptions are as follows:

*First assumption.* The temperature along Z, i.e. normal to the glass plates, is nearly constant within thin (10–20 microns) LC films. However, as noted, in some cases depending on the thickness and nature of the glass plates forming the cells, the temperature can be lower in their vicinity.

*Second assumption.* The phase transition temperature  $T_{N-Sm\ C}$  is HIGHER in the middle part of the samples and LOWER in the vicinity of the glass plates, where a strong realignment in the nematic orientation takes place: the orientation of the LC molecules is changed from planar to homeotropic along a distance which is in the range of several microns. Indeed, during the performance of the experimental investigations it was clarified that the Sm C phase is nucleated first in the middle part of the nematic films followed by Sm C formation in the boundary regions (Figure 8). We find evidence for this important fact in polycrystalline Sm C formation with Sm C local crystals being randomly distributed relative to the glass plate normal (note that in some cases one can observe some ordering in the Sm C monodomains which is attributed to the direction of the temperature gradient or to other non-controlled and unknown forces) (Figure 3). The different brightness of the Sm C monodomains in Figures 3, 4 and 5 (the photos have been taken under parallel nicols) clearly show that the LC molecules very often have different azimuthal orientation either in the various Sm C monodomains or even inside some of them; this is related to the continuous change of this orientation. (At this point it is important to stress that the growing of the Sm C phase from the boundaries to the middle part of strong  $\theta$ ,  $\varphi$ -anchored thin (10–20 microns) planar non-deformed or electrically-deformed nematic films

would be in the form of two types of local Sm C monodomains situated approximately at an angle of  $45^\circ$  relative to the rubbing axis: the Sm C molecules should follow the “easy” axis whereas the Sm C layers should be perpendicular to or inclined to the glass plates).

We find justification for this assumption also in an analogy with the lowering in the transition temperature  $T_{N-Sm A}$  under elastic strains<sup>1</sup> as well as in a number of theoretical<sup>47,48</sup> and experimental results<sup>49,50</sup> predicting and demonstrating respectively the significant enhancement of all three elastic coefficient of splay, twist and bend near the N–Sm C phase transition. Accordingly, the transition temperature in the strongly-deformed boundary regions should be depressed in the presence of bend, twist and splay deformations. When the LC deformations are larger (high electric fields, strong surface anchoring, small coherent lengths) the transition temperature is more depressed.<sup>1</sup> The divergence of the elastic coefficients of bend ( $K_{33}$ ), twist ( $K_{22}$ ) and splay ( $K_{11}$ ) near the N–Sm C phase transition is accompanied by a considerable decrease in the transition temperature. Consequently, the transition temperature in the strongly-realigned boundary regions  $T_{N-Sm C}^b$  will be LOWER than the transition temperature  $T_{N-Sm C}^m$  in the middle region, which is well-aligned by the electric torques, by an amount proportional to  $\text{rot } \vec{n}$  and  $\text{div } \vec{n}$ . The enhancement of the elastic coefficients in some cases characterized by a relatively wide N–Sm C phase coexistence, small latent heat change compared with  $kT$  and either a second-order phase transition or a slightly first-order one<sup>1</sup> results in the occurrence of well-defined pre-transitional stripes already observed in Sm A<sup>1</sup> and Sm C<sup>14</sup> liquid crystals. The gradient in the bend-twist-splay deformations in the N phase together with the rate of cooling can determine the periodicity of the “striped structure”.

The pre-transitional stripes observed during the investigations of many NOBA films clearly pointed out the enhancement of all the NOBA elastic nematic coefficients. In addition, the latent heat change at the N–Sm C phase transition for the liquid crystal NOBA measured in 1967 by Herbert<sup>51</sup> to be around 0.04 cal/g is very small and comparable to that peculiar to the N–Sm A phase transition for CBOOA which has been measured to be between 0.06 and 0.10 cal/g.<sup>1,52</sup> Moreover, the increase in electric field strength led to a considerable decrease of the stripe period. This situation is further complicated by the rapid cooling of the samples in the range of  $15^\circ\text{C}/\text{min}$ , which according to Luckhurst, Ptak and Sanson<sup>26</sup> can change the type of the phase transition. (Cladis and Torza pointed out that the N–Sm A phase transition for CBOOA liquid crystal is a first order transition<sup>53</sup>.) Furthermore, the strong electric field applied across

the samples under study between  $15 \times 10^3$  V/cm and  $15 \times 10^4$  V/cm is able to change the transition temperature  $T_{N-Sm\ C}$  of even the completely oriented nematic phase in the middle part of the cells (the change in the phase transition temperature of well-aligned LCs has been investigated to date, according to our knowledge, only for the case of N-Sm A phase transition and the results have been contradictory as follows: theoretical predictions show a rise in the transition temperature<sup>54</sup> whereas the experimental results obtained by Sakamoto *et al.* pointed to a considerable decrease in this temperature<sup>55</sup> which is in accordance with Helfrich's theory<sup>56</sup> taking into account the magnitude and sign of the dielectric constants of both phases). However, direct measurements of the difference between the phase transition temperatures in the middle part of the samples and in the boundary regions, at the present stage of experimental investigation, are not possible, and only the physical considerations based on the optical properties of the textures observed can give the correct answer (note, that this problem can be successfully resolved by means of a transversal electric field when the LC orientation can be governed by surface forces generated from the electrodes).

All considerations show that the Sm C phase arises first in the middle homeotropic part of the samples with a growth of skewed cybotactic groups.<sup>33, 57, 58</sup>

*Third assumption.* The final orientation of the Sm C layers is determined by the corresponding orientation of the Sm C molecules and layers in the cybotactic groups just before the N-Sm C phase transition.

This assumption is based on the fact that the Sm C phase is formed after a divergence in the size of the cybotactic groups: i.e. the orientation of the Sm C molecules and layers in these groups cannot be ignored. At this point we must emphasize the possible orientation of the Sm C layers. Most of the authors dealt with the existence of the cybotactic groups in the nematic phase of LCs with N to Sm C phase transition unambiguously pointed out their skewed character.<sup>33, 57, 58, 59-66</sup> Other authors, however, pointed out the normal position of the smectic planes,<sup>67, 68</sup> i.e., the existence of a Sm A structure inside each cybotactic group.<sup>68</sup> Of special importance are the assumptions of Chou and Carr<sup>13</sup> and of Rao *et al.*<sup>69</sup> made on the basis of either conductivity measurements or by EPR investigations about a Sm A structure in the nematic phase of the liquid crystal NOBA.

The two possible orientations of the smectic layers in the cybotactic groups formed in the middle part of the samples, where the nematic

phase is homeotropic, are shown in Figures 11a and 11b. It is natural to assume that the orientation of the LC molecules in the cybotactic groups is homeotropic since the dielectric torques due to Sm A or Sm C arrangements (negative sign of the dielectric anisotropy) are negligibly weak: the number of the molecules in the cybotactic groups in the range of 100 is by far not sufficient to ensure the orienting action of the electric field.<sup>34</sup> The influence of the electric field on the cybotactic groups, in effect, is indirect and is effected by the action of the remaining nematic phase in agreement with Meiboom and Hewitt's experimental results.<sup>70</sup>

Although we are inclined to accept that the Sm C arrangement is more likely in the cybotactic groups, it should be noted that the passing from normal cybotactic groups with a Sm A arrangement of the LC molecules to skewed cybotactic groups with a Sm C arrangement is possible with a slipping of the molecules, as has often been observed after the Sm A–Sm C phase transition under the action of various electric,<sup>71</sup> magnetic<sup>72</sup> or surface forces.<sup>73,74</sup> However, it is reasonable to accept Sm C orientation of the LC molecules in the cybotactic groups just before the N–Sm C phase transition where both the N and Sm C phases coexist. In addition, the LC molecules should be homeotropic and the orientation of the Sm C layers oblique. Two of the infinitely possible positions of the Sm C layers are shown in Figure 11b. The Sm C layers are inclined relative to the glass plate normal at an angle of approximately  $45^\circ$ , the characteristic temperature independent tilt angle for the NOBA Sm C liquid crystal. It is clear that all Sm C layer normals make a cone with an apex angle

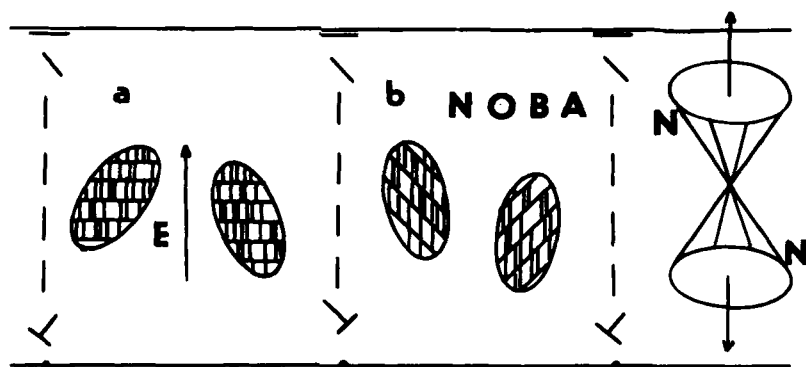


FIGURE 11 Two possible orientations of the smectic layers in the cybotactic groups formed after rapid cooling in the middle part of thin twisted nematic NOBA films: (a) Sm A arrangement; (b) one Sm C arrangement from the infinitely possible ones; a cone made by all possible normals to the Sm C layers has been shown as well.

equal to  $90^\circ$  (Figure 11b). According to our third assumption, the Sm C layers maintain their oblique position relative to the glass plates after the N-Sm C phase transition (Figure 12a).

Note that the Sm C phase formed in the middle part of the samples is insensitive to the influence of the surface forces, since it is apparently separated from the two glass plates by two very thin, with a thickness of several microns, nematic films with cybotactic groups: see the schematic representation of the possible N and Sm C textures observed, as given in Figure 8. This assumption is confirmed by the formation, for the first time in our experiment, of a number of Sm C monodomains with an oblique position of the Sm C layers relative to the glass plates (to date such Sm C monodomains have been obtained only either under the action of strong polar and azimuthal surface forces in thin films or under the action of magnetic or electric fields applied across the LCs in tubes with a diameter of several millimeters<sup>26,70</sup>).

The importance of the boundary conditions being able to determine not only the orientation of the Sm C molecules and layers but also the possible kind of the Sm C textures, has been demonstrated in our experiment by the rapid cooling of a homeotropic nematic phase in the presence of a high a.c. electric field, which is stabilizing in the nematic phase and destabilizing in the Sm C phase (note that the LC in the middle part of the cells being investigated had been under the same action of the electric field). The final result was the formation of blurred shaped Schlieren textures without the creation of any monodomains with an oblique orientation of the Sm C layers.

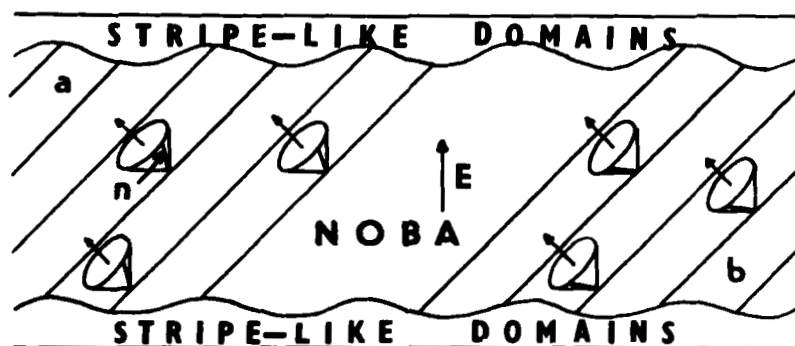


FIGURE 12 One orientation (among the infinite possibilities) of the Sm C molecules and layers according to our model: (a) initial normal position of the Sm C molecules; (b) final planar position of the Sm C molecules, which is achieved under the action of the dielectric torques (negative sign of the dielectric anisotropy of the Sm C phase).

*Fourth assumption.* The Sm C molecules go from a homeotropic to planar position under the action of the dielectric torques of the Sm C phase (negative value of the dielectric anisotropy) (Figure 12b).

This kind of probably thresholdless dielectric transition, which is realized without any resistance of the elastic forces, is expected for large Sm C monodomains and has already been proposed for the magnetic case.<sup>75,76</sup> Indeed such a reorientation of the Sm C NOBA molecules in the presence of a high electric field between 5000 V/cm and 7000 V/cm was observed by Chou and Carr a long time ago;<sup>13,77</sup> we stress at this point that the electric field applied across the N and Sm C films in our experiment had a magnitude above 1500 V/cm.

(b) Alignment of the Sm C phase in the boundary regions of the samples: matching of the bulk Sm C orientation.

The matching of the Sm C LC formed in the middle part of the cells under study with that formed in the boundary regions is characterized by the creation of different kinds of inversion walls and edge-dislocations. One can observe various types of the usual tilt-inversion walls without any undulation, compression or dilation of the Sm C layers and various types of edge-dislocation lines. The usual tilt-inversion walls (designated by A in Figure 4) as noted were rarely observed when the voltage applied across the N and Sm C phases was relatively low. The most frequent objects (designated by B in Figure 4 and all the textures observable in Figure 5) obtained during the experimental investigations were interpreted to be various novel Sm C edge-dislocations with a very large Burger vector formed for the first time in planar Sm C films (one example from the infinite possibilities for edge-dislocation lines and the corresponding orientation of the Sm C layers in the middle part of the cells is schematically shown in Figure

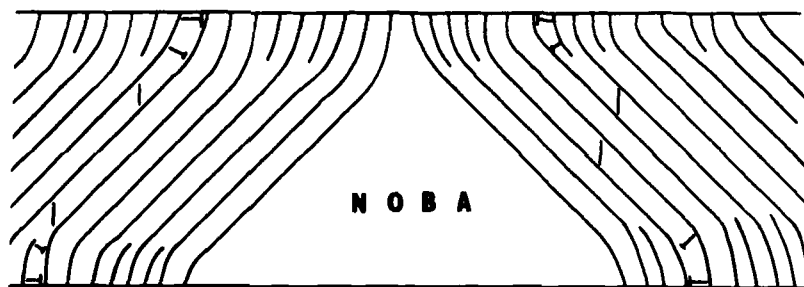


FIGURE 13 One example (among the infinite possibilities) of a topological model showing the dislocation lines in thin Sm C samples with an oblique position of the Sm C layers in the middle part and a complex splay-twist-bend realignment of the Sm C molecules in the boundary regions.



13). Justification for this important assumption is found in the oblique position of the Sm C layers relative to the glass plates and in the optical properties of the objects observed being very similar to those of the dislocation tilted walls obtained and investigated in detail by Williams and Kléman in Sm A<sup>39-41</sup> as follows:

(i). One usually observe very sharp dark and broader bright lines adjacent to each other which do not depend significantly on the various possible position of the nicols related to the strong refraction and even total internal reflection of the light from the edge-dislocation lines due to the strong variation of the optical indices in these regions.

(ii). The dislocation lines parallel to the Sm C planes are localized near the glass plates which results in their relief being very clear and distinct.

(iii). The inclination of the Sm C layers in the middle part of the films together with the account of both the initial twist in the nematic phase and the ability of the LC under study to form cybotactic groups easily can lead to a significant bending of the Sm C layers and to the creation of dislocation lines. This bending of the Sm C layers accompanied by complex bend-twist-splay deformations of the Sm C molecules inside each of the Sm C layers (Figure 13) is confirmed by the strong influence of the optical pictures by variations in the electric field magnitude even in the Sm C phase: we stress here that the small dielectric anisotropy of the NOBA Sm C liquid crystal in the range of  $(-0.025)$  together with the relatively low magnitude of the voltage applied across the cells between  $80 V_{\text{eff}}$  and  $300 V_{\text{eff}}$  is not able to cause even weak deformations of the Sm C layers.

(iv). The edge-dislocation lines can be created in some cases by other non-energetic causes, such as the manner of Sm C nucleation and strong temperature gradients, etc.

(v). An increase of the voltage up to  $300 V_{\text{eff}}$ , i.e. 10 times the threshold voltage, leads not only to a decrease in the dislocation period but also to a decrease in the penetration depth of the dislocation walls into the middle part of the films.

(vi). Although the dislocation walls in the Sm C phase are more complex due to the very realignment of the Sm C molecules inside the Sm C layers, it seems that the bright part of the dislocation walls is on the compressed side of the dislocations, whereas the dark part is on dilated side of the same dislocation.<sup>39-41</sup>

(vii). Edge-dislocation lines cannot be obtained after the rapid cooling of twisted nematic films down to the Sm C phase when the Sm C layers are parallel to the glass plates due to the possibilities existing for easy adaption of the twist deformation (see the experimental results obtained by Arora *et al.*<sup>24</sup>).

Indeed, in some cases, one notes two or more possibilities for the eventual interpretation of the objects observed such as dislocation walls, and Sm C layer undulations, etc., and it is difficult to prefer one of them. However, this problem exists for the Sm A case as well and only clear physical considerations or additional experimental investigations can lead to a correct interpretation.

c) Possible physical causes leading to the formation of edge-dislocations in the Sm C phase.

To understand the formation of edge-dislocations in the Sm C phase it is necessary to discuss the influence of the various parameters which can play an essential role in the phenomenon under study, such as the existence of twist in the boundary regions (let us remember that the matching of the same Sm C phase grown from an electrically-realigned planar N film to that formed in the boundary regions has been effected by the formation of oblique Sm C layers just up to the glass plates without the creation of any kind of edge-dislocation lines or various types of tilted-inversion walls), the eventual role of the surface coupling of the Sm C films under study and finally, the possible type of N-Sm C phase transition coupled to the rate of cooling.<sup>26</sup>

(i). Possible role of the twist deformation in the boundary regions of the cells in both the N and Sm C phase for the creation of edge-dislocation in the Sm C phase

The boundary regions of the electrically-realigned twisted N cells were modeled by the construction of thin (2–3 microns) twisted cells, which was achieved without the utilization of spacers. Upon cooling these cells, pronounced pre-transitional stripes that were apparently linked with the enhancement of the N twist elastic coefficient were observed just above the N-Sm C phase transition. The further cooling of the cells below the N-Sm C phase transition led to the creation of both the various Sm C monodomains with different inclination of the Sm C molecules relative to the glass plates, which is indicated by the creation of  $\pi$ -inversion walls accompanied by pronounced colouring of adjacent Sm C monodomains, and edge-dislocation lines which are very similar to those already observed by Lagerwall *et al.* in wedge-shaped Sm C films.<sup>42–45</sup>

It is worth mentioning that the rapid cooling of thin (2–3 microns) hybrid-aligned planar-homeotropic N NOBA films down to the Sm C phase always led to the formation of homogeneously-oriented Sm C films with many open and loop  $\pi$ -inversion walls. In addition, the Sm C molecules in such cells were always oriented along the rubbing direction determining the LC orientation at one of the surfaces (the other surface was coated by lecithin to give a homeotropic orientation of the LC molecules).

However, twist deformations might be induced in the boundary regions of the electrically-realigned planar N films upon cooling as well, due to the action of the Sm C phase already formed in the middle part of the samples: Sm C single crystals which are randomly-distributed relative to the glass plate normal may determine a different azimuthal orientation of the Sm C molecules after the electric field realignment. It seems that at least two essential reasons make the creation of such a Sm C-induced twist difficult: the first reason is connected with the possibilities for a higher transition temperature in the boundary regions of electrically-realigned PLANAR nematic films on comparison with that characteristic for electrically-realigned TWISTED N films, due to the lack of a boundary-induced twist (the details of Sm C formation in the different regions of such cell are not clear), and the second one is related to the possible role of the cybotactic groups formed in the NON-TWISTED nematic boundary regions. Whatever the reason, the final experimental result is that such Sm C-induced twisting is not capable of promoting the generation of surface-induced edge-dislocations.

(ii). Possible role of the surface coupling in both the N and Sm C phases for the creation of edge-dislocations in the Sm C phase

The important role of the  $\theta$ -polar and  $\varphi$ -azimuthal surface anchoring (Figure 7) in determining different orientations of the Sm C molecules and layers has already been noted at the beginning of this paper. It is interesting to point out that the Sm C phase in the boundary regions is actually formed under the influence of strong surface forces due only to one of the glass plates. On the other side of the interfacial LC layer, natural Sm C surface forces generated from the previously-formed Sm C phase in the middle part of the samples act, which can dictate the formation of the Sm C phase in the boundary regions. It is evident that the various kinds of edge-dislocation walls can be generated only under the action of strong  $\varphi$ -azimuthal surface forces, which usually overcome the  $\theta$ -polar ones. The various Sm C textures observed during our experimental investigations clearly indicate that the smectic  $\varphi$ -azimuthal and  $\theta$ -polar surface energies are not equal and may vary from one region of the glass plates to another. For instance, it is possible to obtain the usual tilted-inversion walls, various dislocation lines and even non-deformed Sm C monodomains experimentally (Figs. 4 and 5), depending on the strength of both surface forces and dielectric torques.

We are inclined to think that edge-dislocation lines are formed under the combined complex action of the initial twist in the nematic phase, which is closely related to the surface anchoring of the nematic films, the formation of oblique Sm C layers in the middle part of the

samples, the ability of the LC under study to form cybotactic groups easily and finally, the strong  $\varphi$ -azimuthal surface anchoring of the Sm C phase, which however, is itself not capable of inducing a curving of the Sm C layers with a complex splay-twist-bend realignment of the Sm C molecules.

(iii). Possible role of the cooling rate and the type of the phase transition for the creation of edge-dislocations in the Sm C phase

The type of the N-Sm C phase transition plays a crucial role in the creation of well-defined pre-transitional stripes, which upon cooling can start the novel Sm C textures. Although the N to Sm C phase transition has been pointed out to be of a possible second order,<sup>78</sup> most of the theoretical and experimental results reveal the first-order character of this transition.<sup>47,48,79,80</sup> On the other hand, in analogy with the Sm A case it seems that such pre-transitional stripes can be formed only in the case when the corresponding phase transitions (N-Sm A, N-Sm C etc.) are accompanied by low latent heat, which is typical for second or slightly first-order phase transitions.

As far as the role of the rate of the cooling of the N phase down to the Sm C phase for the creation of edge-dislocations is concerned we may say that this problem can be discussed in two views. The first one has been touched upon by Nesrullaev and Sonin<sup>59</sup> who relate the cooling rate to one of the possible ways for the appearance and growth of the nucleated centers. The second one is connected with the possibility of the cooling rate to change the latent heat, and consequently the type of the phase transition. Indeed, this problem has already been discussed in 1973 by Luckhurst *et al.*<sup>26</sup> For instance, the growth of the Sm C phase from initially very thin (2–3 microns) twisted nematic NOBA films upon very slow cooling clearly shows the absence of pre-transitional stripelike domains and edge-dislocations. This observation clearly points out that the latent heat and consequently the type of the phase transition change with the rate of cooling in the N phase down to the Sm C phase.

(3) Possible relaxation of the dislocation walls and the storage effect.

According to Williams and Kléman<sup>39–41</sup> the edge-dislocation lines in Sm A phase after grouping to form a large Burger vector can relax in the presence of a glass plate boundary into pairs of  $\pi$ -lines and further into focal conics. The situation with Sm C, however, is much more complex. It seems that the edge-dislocations should relax after grouping to form a large Burger vector into Néel walls with a partial twist (we recall that inside the bent Sm C layers there is a strong

splay-twist-bend realignment of the Sm C molecules) and further into a series of alternating nuclei  $s = +1$  and  $s = -1$ .<sup>17, 21, 36, 37, 38</sup> During our experimental investigations, however, only various types of tilted-inversion walls and edge-dislocation walls were obtained. This is probably due to the larger value of the Sm C  $A_{21}$  elastic coefficient relative to  $A_{12}$  as has been shown by our experimental results for the NOBA liquid crystal.

As claimed at the beginning of this work one notes only a slight change in the dislocation walls after the electric field is removed. Consequently, the various types of dislocation lines or walls obtained during the performance of our experiment can be successfully employed as an appropriate storage mode for industrial applications.<sup>81, 82</sup> The major advantages characterizing this novel type of storage mode result in their direct governing by surface forces, independence of the frequency of the voltage applied across both the N and Sm C phases, independences of possible temperature variations inside the Sm C interval and long stability, etc. The last of these advantages is directly confirmed by the existence of some of the dislocation lines in the first optically isotropic crystal phase formed after the Sm C phase upon cooling.

## CONCLUSION

Various kinds of Sm C layer undulation instabilities are obtained after the rapid cooling of twisted, hybrid-aligned and homeotropic NOBA nematic films. The rapid cooling of homeotropic nematic films led to the formation of Sm C stripes following the  $C_2$  axis which are caused by second order effects. On the other hand, the rapid cooling of twisted N films led to the formation of two kinds of Sm C stripes, one following the  $C_2$  axis and produced by second-order effects and the other which is perpendicular to this axis and produced by first-order effects. The magnitude of the stripe period of these Sm C layer undulation instabilities permits the crude estimation of the NOBA Sm C dilation modulus  $\tilde{B}$ , which was measured to be around  $0.32 \times 10^{+4}$  erg/cm<sup>3</sup> and the determination of the larger elastic Sm C coefficient  $A_{21}$  in comparison with  $A_{12}$ .

The application of a high a.c. electric field across both the twisted nematic and Sm C phases, which aligns the N molecules homeotropic (positive value of the dielectric anisotropy) and Sm C molecules planar (negative value of the dielectric anisotropy) may completely remove the Sm C layer undulations and is capable of creating various types of

well-defined and optically-observable edge-dislocation walls (or lines) due to the different orientation of the Sm C molecules and layers in the middle part of the samples being studied and those in the boundary regions. Possible causes, such as the existence of initial twist in the N phase, the strong azimuthal anchoring of the Sm C molecules, the role of the cybotactic groups, the rate of cooling being closely related to the possible type of the phase transition and the orientation of the Sm C layers in the middle part of the samples are discussed in detail. Finally, important problems such as the possible relaxation of edge-dislocation walls and their possible application as a suitable storage mode have been covered.

## References

1. P. E. Cladis and S. Torza, *J. Appl. Phys.*, **46**, 584 (1975).
2. F. J. Kahn, *Appl. Phys. Lett.*, **22**, 386 (1973).
3. H. P. Hinov, *J. Phys. (Paris)*, **42**, 307 (1981).
4. D. Johnson and A. Saupe, *Phys. Rev.*, **A15**, 2079 (1977).
5. T. R. Taylor, J. L. Ferguson and S. L. Arora, *Phys. Rev. Lett.*, **24**, 259 (1970).
6. H. P. Hinov, N. Shonova and K. Avramova, *Mol. Cryst. Liq. Cryst.*, in press (1983).
7. L. E. Hajdo and A. C. Eringen, *J. Opt. Soc. Am.*, 1017 (1979).
8. G. Ryschenkow and M. Kléman, *J. Chem. Phys.*, **64**, 404 (1976).
9. M. Kléman and G. Ryschenkow, *J. Chem. Phys.*, **64**, 413 (1976).
10. E. Guyon and W. Urbach, in "Nonemissive Electrooptic Displays," Ed. by A. R. Kmetz and F. K. von Willisen, Plenum Press, 121 (1976).
11. Z. Kh. Kuvatov, A. P. Kapustin and A. N. Trofimov, *Zh. Eksp. Teor. Fiz. Pis. Red.*, **19**, 89 (1974).
12. Z. Kh. Kuvatov, A. P. Kapustin and A. N. Trofimov, "LCs and Their Application in the Practice", Ivanovo, 74 (1976).
13. L. S. Chou and E. F. Carr, *Liq. Cryst. Ord. Fluids*, vol. 2, 39 (1973).
14. T. J. Scheffer, H. Grüler and G. Meier, *Sol. St. Comm.*, **11**, 253 (1972).
15. R. Bartolino and G. Durand, *Ann. Phys.*, **3**, 257 (1978).
16. S. Kumar, *Phys. Rev.*, **A23**, 3207 (1981).
17. L. Bourdon, J. Sommeria and M. Kléman, *J. Phys. (Paris)*, **43**, 77 (1982).
18. D. Demus and L. Richter, "Textures of Liquid Crystals", VEB Deutch. Ver. Grundsoffind., Leipzig (1978).
19. D. Demus, *Krist. Tech.*, **10**, 933 (1975).
20. F. Rondelez, W. Urbach and H. Hervet, *Phys. Rev. Lett.*, **41**, 1058 (1978).
21. C. Allet, M. Kléman and P. Vidal, *J. Phys. (Paris)*, **39**, 181 (1978).
22. W. Urbach, M. Boix and E. Guyon, *Appl. Phys. Lett.*, **25**, 479 (1974).
23. T. R. Taylor, S. L. Arora and J. L. Ferguson, *Phys. Rev. Lett.*, **25**, 722 (1970).
24. S. L. Arora, J. L. Ferguson and A. Saupe, *Mol. Cryst. Liq. Cryst.*, **10**, 243 (1970).
25. C. R. Luckhurst and A. Sanson, *Mol. Cryst. Liq. Cryst.*, **16**, 179 (1972).
26. G. R. Luckhurst, M. Ptak and A. Sanson, *J. Chem. Soc., Far. Tr.*, **II69**, 1752 (1973).
27. S. Sakagami, A. Takase, M. Nakamizo and H. Kakiyama, *Mol. Cryst. Liq. Cryst.*, **19**, 303 (1973).
28. E. P. Price and Ch. S. Bak, *Mol. Cryst. Liq. Cryst.*, **29**, 225 (1975).
29. V. Tsvetkov, Ph. Dr. Thesis, Institute of Radioelectronics, Moscow (1974).
30. H. P. Hinov, *Mol. Cryst. Liq. Cryst.*, **74**, 1789 (1981).
31. A. Perez, M. Brunet and O. Parodi, *J. Phys. Lett. (Paris)*, **39**, L-353 (1978).
32. D. F. Aliev and A. Kh. Zheinaly, *Zh. Eksp. Teor. Fiz.*, **78**, 2349 (1980).
33. A de Vries, *Pramana Suppl.*, no 1, 93 (1975).

34. P. G. de Gennes, "The Physics of Liquid Crystals", Clarendon Press, Oxford (1974).
35. M. Kléman and L. Lejcek, *Phil. Mag.*, **A42**, 671 (1980).
36. M. Kléman, "Points. Lignes. Parois", Tome I, Ed. de Physique, Paris (1977).
37. M. Kléman, "Points. Lignes. Parois", Tome II, Ed. de Physique, Paris (1978).
38. Y. Bouligand and M. Kléman, *J. Phys. (Paris)*, **40**, 79 (1979).
39. C. E. Williams, Ph. Dr. Thesis, Orsay, Fr. (1976).
40. C. E. Williams and M. Kléman, *J. Phys. Lett. (Paris)*, **35**, L-33 (1974).
41. C. E. Williams and M. Kléman, *J. Phys. Colloq. (Paris)*, **36**, C1-315 (1975).
42. S. T. Lagerwall, R. B. Meyer and B. Stebler, *Ann. Phys.*, **3**, 249 (1978).
43. R. B. Meyer, B. Stebler and S. T. Lagerwall, *Phys. Rev. Lett.*, **41**, 1393 (1978).
44. S. T. Lagerwall and B. Stebler, *Phys. Bull.*, **31**, 349 (1980).
45. S. T. Lagerwall and B. Stebler, *J. Phys. Colloq. (Paris)*, **40**, C3-53 (1979).
46. M. Lefèvre, J.-L. Martinand, G. Durand and M. Veyssie, *C. R.-Sc. Acad. Paris*, **B273**, 403 (1971).
47. J. Chen and T. C. Lubensky, *Phys. Rev.*, **A14**, 1202 (1976).
48. K. C. Chu and W. C. McMillan, *Phys. Rev.*, **A15**, 1181 (1977).
49. H. Grüler, *Z. Nat.*, **28a**, 474 (1973).
50. H. Grüler and G. Meier, *Mol. Cryst. Liq. Cryst.*, **23**, 261 (1973).
51. A. S. Herbert, *Trans. Far. Soc.*, **63**, 555 (1967).
52. F. Hardouin, H. Gasparoux and P. Delhaes, *J. Phys. Colloq. (Paris)*, **36**, C1-127 (1975).
53. S. Torza and P. E. Cladis, *Phys. Rev. Lett.*, **32**, 1406 (1974).
54. C. Rosenblatt, *J. Phys. Lett. (Paris)*, **42**, L-9 (1981).
55. A. Sakamoto, K. Yoshino, U. Kubo and Y. Inuishi, *Jpn. J. Appl. Phys.*, **15**, 545 (1976).
56. W. Helfrich, *Phys. Rev. Lett.*, **24**, 201 (1970).
57. A. de Vries, *J. Phys. Colloq. (Paris)*, **36**, C1-1 (1975).
58. A. de Vries, *Mol. Cryst. Liq. Cryst.*, **10**, 219 (1970).
59. W. L. McMillan, *Phys. Rev.*, **A8**, 328 (1973).
60. F. Rondelez, *Sol. St. Comm.*, **11**, 1675 (1972).
61. F. Rondelez, Ph. Dr. Thesis, *Philips Res. Repts. Suppl.*, **2**, 121 (1974).
62. A. L. Berman, E. Gelerinter and A. de Vries, *Mol. Cryst. Liq. Cryst.*, **33**, 55 (1976).
63. K. U. Deniz, A. S. Paranjpe, E. B. Mirza, P. S. Parvathanathan and K. S. Patel, *J. Phys. Colloq. (Paris)*, **40**, C3-136 (1979).
64. A. de Vries and S. B. Qadri, *Proc. Int. Conf. LCs*, Bangalore, India (1979).
65. A. J. Leadbetter and E. K. Norris, *Mol. Phys.*, **38**, 669 (1979).
66. V. M. Setha, A. de Vries and N. Spielberg, *Mol. Cryst. Liq. Cryst.*, **62**, 141 (1980).
67. V. Azaroff, *Proc. Nat. Acad. Sci. USA*, **77**, 1252 (1980).
68. H. Terauchi, *J. Phys. Colloq. (Paris)*, C3-401 (1979).
69. A. S. N. Rao, P. N. Murty and T. R. Reddy, *Phys. Stat. Sol.*, **a68**, 373 (1981).
70. S. Meiboom and R. C. Hewitt, *Phys. Rev. Lett.*, **34**, 1146 (1975).
71. H. Kresse, A. Wiegeleben and D. Demus, *Krist. Tech.*, **15**, 341 (1980).
72. C. R. Safinya, M. Kaplan, J. Als-Nielsen, R. J. Birgeneau, D. Davidov and J. D. Litster, *Phys. Rev.*, **B21**, 4149 (1980).
73. T. E. Lockhart, D. W. Allender, E. Gelerinter and D. L. Johnson, *Phys. Rev.*, **A20**, 165 (1979).
74. K. C. Lim and J. T. Ho, *Phys. Rev. Lett.*, **40**, 1576 (1978).
75. R. M. Hornreich and S. Shtrikman, *Sol. St. Comm.*, **17**, 114 (1975).
76. L. Benguigui and D. Cabib, *Phys. Stat. Sol.*, **a47**, 71 (1978).
77. L. S. Chou and E. F. Carr, *Phys. Rev.*, **A7**, 1639 (1973).
78. P. G. de Gennes, *Mol. Cryst. Liq. Cryst.*, **21**, 49 (1973).
79. R. De Hoff, R. Biggers, D. Brisbin and D. Johnson, *Phys. Rev.*, **A25**, 472 (1982).
80. A. Nesrullaev and A. Sonin, *Zh. Phys. Chim.*, **LIII**, 2481 (1979).
81. M. P. Petrov, B. P. Petroff and P. Simova, *Compt. Rend. Acad. Bulg. Sci.*, **31**, 647 (1978).
82. P. Simova and M. Petrov, *Mol. Cryst. Liq. Cryst.*, **74**, 1875 (1981).